PROCEEDINGS OF THE INTERNATIONAL CONFERENCE
NANOMATERIALS: APPLICATIONS AND PROPERTIES
Vol. **2** No 4, 04NAESP04(4pp) (2013)

Ultrathin Photovoltaic Donor-Acceptor Structure with Opposite Built-in Fields

L.M. Blinov*, V.V. Lazarev, S.G. Yudin

Shubnikov Institute of Crystallography, Russ. Acad. Sci, 59, Leninsky Prosp., 119333 Moscow, Russian Federation

(Received 19 April 2013; published online 29 August 2013)

We discuss organic heterostructures, in which ultrathin layers of an organic material alternate with layers of other organic materials, such as dyes, organic semiconductors or ferroelectric polymers. The study is focused on the distribution of an external electric field and the measurements of the built-in-fields in the donor and acceptor layers within photovoltaic heterostructures. The built-in-fields play an extremely important role in development of organic solar cells, photodetectors, LEDs, transistors, etc. Our investigations are based on the electroabsorption (or Stark spectroscopy) technique. As an example, built-in fields were studied on an organic solar cell heterostructure ITO-CuPc-C_{60}-Al. Two strong built-in fields of opposite directions have unexpectedly been found in the bulk of the donor (copper phthalocyanine, CuPc) and acceptor (fullerene, C_{60}) layers under equilibrium conditions. Such a phenomenon has not been observed earlier and owes to the particular accumulation of excess holes trapped at the CuPc / C_{60} interface.

Keywords: Nanostructured films, Optical properties, Organic photovoltaics.

PACS numbers: 73.50.Pz, 73.30. + y, 78.66.Qn

1. INTRODUCTION

Nowadays power conversion efficiency of solar cells reaches 30 % for inorganic and about 10 % for organic materials but these parameters do not meet the economic demands yet. Note that organic materials are much cheaper than inorganic ones and have other advantages, in particular, they are light, could be flexible and compatible with printing technology. Many groups all over the world work on improvement of organic solar cells [1-3], however, there is no yet fundamental understanding the physical processes going on in multilayered organic heterostructures. One of serious problems is a measurement of an internal, built-in field formed spontaneously in asymmetric heterostructures supplied with metal electrodes with different work functions. It is the field that is responsible for the dissociation of excitons after light absorption by an organic semiconductor and the subsequent drift of charge carriers to electrodes. The built-in field E_b can be measured using a compensation of the light induced current by an external d.c. voltage $U_0 \approx d \cdot E_b$, where d is total thickness of the heterostructure between electrodes [4]. In that case, one gets only a value of $\langle E_b \rangle$ averaged over the heterostructure. In fact, only spectroscopic technique of electroabsorption allows us to obtain information on the field E_b in each elements of a heterostructure. The basic advantage of electroabsorption techniques [5-8] is a possibility to measure spectral shifts simultaneously on the two frequencies (1ω and 2ω) of an applied probe a.c. field $U = U_m \sin\omega t$ without an external d.c. field and strong illumination. It is a comparison of the electroabsorption spectra at frequencies of 1ω and 2ω that allows us to find an amplitude and direction of the built-in fields in each elements of the heterostructure under investigations.

2. HETEROSTRUCTURE ITO-CuPc-C_{60}-Al

2.1 Samples

Here we investigate a heterostructure ITO-CuPc-C_{60}-Al consisted of a donor layer of copper phthalocyanine (CuPc) and an acceptor layer of fullerene (C_{60}) placed between transparent $(In_xSb_{1-x})_2O_3$ (ITO) and semitransparent (Al) electrodes. The work functions of all elements separated from each other are shown in Inset to Fig. 2.1.

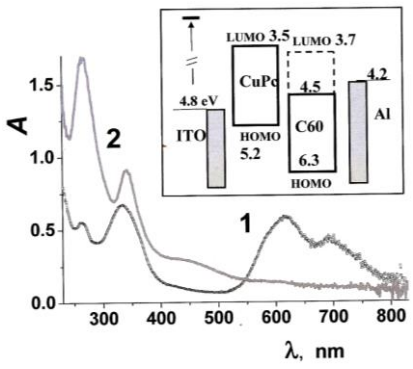

Fig. 2.1 – Inset: Diagram of work functions [1, 10] for the elements of the heterostructure studied. For CuPc the bandwidth between HOMO and LUMO is 1.7 eV; in the case of C_{60} film, there are charge transfer states weakly allowed by symmetry that reduce the width of forbidden band from 2.6 eV to 1.8 eV [11]; Main plot: Spectra of absorbance for 55 nm thick CuPc layer (black curve 1) and 70 nm thick C_{60} layer (gray curve 2)

This heterostructure is a simplified version of well-known solar cells [9], in which hole and electron transport layers adjacent to the electrodes are absent. In this case, the electroabsorption spectra reveal directly built-in fields in the bulk of the donor and acceptor layers. Additionally, there were prepared two samples (Schottky diodes) with individual layers of CuPc and C_{60}, each between the same ITO and Al electrodes. All samples were prepared by subsequent vacuum evaporation of CuPc, C_{60} and Al on

fused quartz substrates covered with patterned ITO. On each substrate, there were prepared three electroded elements of size 4×4 mm², and remaining place was used for the measurements of CuPc and C_{60} absorbance with CCD spectrometer Avantes-2048. The corresponding spectra are shown in Fig. 2.1. The thickness of the CuPc (55 ± 5 nm) and C_{60} (70 ± 5 nm) layers was found using the calibration spectra of their absorption coefficients measured on thicker etalon samples with a Linnik interferometer (MII-4).

2.2 Electroabsorption

The a.c. electric field $E_m \sin\omega t$ applied to the electrodes causes spectral shifts of all absorption bands by $\Delta\lambda$, dependent on a wavelength λ and differences of dipole moments $\Delta\mu = \mu_e - \mu_g$ and polarizabilities $\Delta\alpha = \alpha_e - \alpha_g$ between an excited (index e) and the ground (index g) states of a molecule [12]. As a result, the absorbance spectrum $A(\lambda)$ is also changed by $\Delta A_m(\lambda) = -(\Delta T_m / T)/\ln 10$ where $T(\lambda)$ is optical transmission spectrum of the sample with electrodes. For a centrosymmetrical, isotropic film placed between identical electrodes $\Delta A(\lambda)$ is quadratic-in-field and can only be observed at the double frequency (2ω) of an applied field of frequency ω [5, 6, 13]. For each individual band the increment $\Delta A(\lambda)$ at 2ω is given by:

$$\Delta A_{m,2\omega}(\lambda) = -\frac{1}{2} E_m^2 \left(\frac{\varepsilon+2}{3}\right)^2 \times \times \left[\frac{\lambda^4 (\Delta\mu)^2}{10(hc)^2}\frac{\partial^2 A}{\partial\lambda^2} - \frac{\lambda^2 \Delta\alpha}{2hc}\frac{\partial A}{\partial\lambda}\right] \equiv -\frac{1}{2}\left(\frac{\varepsilon+2}{3}\right)^2 E_{m,2\omega}^2 F(\lambda) \quad (2.1)$$

where h and c are Planck's constant and free space light velocity, $(\varepsilon + 2)/3$ is the Lorentz local field factor with dielectric permittivity ε of the film, $\Delta\mu$ and $\Delta\alpha$ are parameters of the molecular absorption bands under discussion. Generally, for non-centrosymmetrical heterostructures one observes both quadratic and linear response at frequencies 2ω and 1ω, respectively. However, if only centrosymmetrical substances (no ferro- or pyroelectric components) are placed between *different electrodes*, the linear effect is caused either by a built-in field E_b or a d.c. field E_0 from an external source. Only in this particular case, the electroabsorption spectra at 2ω and 1ω have exactly the same shape but differ by amplitudes and can differ by signs. It means that "molecular" function $F(\lambda)$ in Eq. (2.1) is identical for both spectra. Indeed, the last term in Eq. (2.2)

$$(E_0 + E_b + E_m \sin\omega t)^2 = (E_0 + E_b)^2 + (1/2)E_m^2 + +2(E_0 + E_b)E_m \sin\omega t - (1/2)E_m^2 \cos 2\omega t \quad (2.2)$$

corresponds to $\Delta A_{m,2\omega}(\lambda)$ spectrum, while the electroabsorption spectrum measured at the fundamental frequency ω is given by

$$\Delta A_{m,\omega}(\lambda) = 2\left(\frac{\varepsilon+2}{3}\right)^2 (E_0 + E_b)E_m F(\lambda) \quad (2.3)$$

From the ratio of equations (2.3) and (2.1) in the absence of the external d.c. voltage ($E_0 = 0$) we get the amplitude of the built-in field

$$E_b = -\frac{E_m}{4} \cdot \frac{\Delta A_{m,\omega}}{\Delta A_{m,2\omega}} \quad (2.4)$$

usually measured at a wavelength of the maximal signal/noise ratio. This simple analysis of electroabsorption for a single spectral band is also valid for a set of overlapped bands which, if necessary, may be represented by a sum of several Gaussians [13].

2.3 Built-in Fields in Individual Layers

The three mentioned samples were transparent enough for detecting electroabsorption signals within λ = 300-800 nm using a Xenon lamp, a monochromator, a photomultiplier and an automated device [6] for the phase-sensitive spectral measurements of $\Delta A_{m,\omega}(\lambda)$ and $\Delta A_{m,2\omega}(\lambda)$.

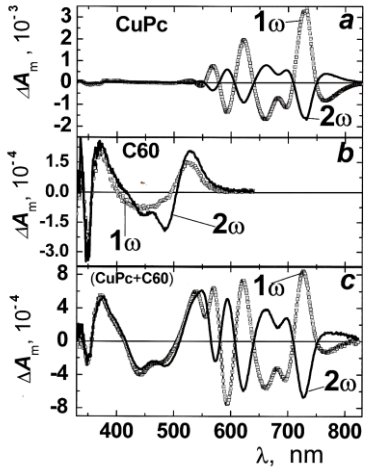

Fig. 2.2 – Electroabsorption spectra at frequency 1ω and 2ω of an applied a.c. voltage $U_m \sin\omega t$ at $f = \omega/2\pi = 30$ Hz: (a) sample of copper phthalocyanine ITO-CuPc-Al, $U_m = 4$ V; (b) sample of fullerene ITO-C_{60}-Al, $U_m = 4$ V; (c) heterostructure ITO-CuPc-C60-Al, $U_m = 8$ V

The spectra of electroabsorption for layers of individual materials CuPc and C_{60} are shown in Fig. 2.2a and b, respectively. It is clearly seen that the two curves (1ω and 2ω) in the CuPc spectra have the opposite signs whereas for C_{60} the signs of 1ω and 2ω curves are the same. The amplitude of the applied a.c. voltage ($U_m = 4$ V) and thickness of both samples ($d = 55$ nm for CuPc and 70 nm for C_{60}) are known and, neglecting a high capacitance of thin near-contact layers, we find the amplitudes $E_m = U_m / d$ of the applied a.c. field in the bulk of the layers of CuPc ($E_m = 73$ V/μm) and C_{60} ($E_m = 57$ V/μm). Now, by comparing the maximum amplitudes $\Delta A_{m,2\omega}$ and $\Delta A_{m,\omega}$ at the wavelengths $\lambda = 728$ nm in Fig. 2.2a and $\lambda = 368$ nm in Fig. 2.2b and with the help of Eq. (2.4)

Table – Parameters of CuPc and C_{60} layers in heterostructure ITO-CuPc-C_{60}-Al

	d, nm	E_m, V/μm	λ, nm	$\Delta A_m(1\omega)$	$\Delta A_m(2\omega)$	F, (μ/m)^2	E_b,V/μm	U_b, V
CuPc	55	47	727	$8.4\cdot10^{-4}$	$-6.7\cdot10^{-4}$	$1.51\cdot10^{-7}$	14.73	0.81
C60	70	82.5	373	$5.5\cdot10^{-4}$	$5.2\cdot10^{-4}$	$3.25\cdot10^{-8}$	– 21.8	– 1.53

the amplitudes of the built-in fields are found to be opposite in the two individual samples: $E_b = 37$ V/μm (for CuPc) and $E_b = -11$ V/μm (for C_{60}). The direction of the built-in fields was confirmed by applying a low external voltage $U_0 = \pm 1$ V with respect to the grounded ITO electrode in line with Eq. (2.3). It is found that E_b is directed from Al to ITO electrode in structure ITO-CuPc-Al and from ITO to Al electrode in structure ITO-C_{60}-Al.

Further, with the help of known a.c. fields E_m in layers of CuPc ($\varepsilon = 4$) and C_{60} ($\varepsilon = 4.5$) and using the values of absorbance increments at the double frequency $\Delta A_m(2\omega, E, \lambda)$ at the same $\lambda = 728$ nm (CuPc) and $\lambda = 368$ nm (C_{60}), we can find the values of "molecular" factor F in Eq. (2.1) for both materials: $F1 = 1.5\cdot10^{-7}$ μm/V^2 (for CuPc) and $F2 = 3.25\cdot10^{-8}$ μm/V^2 (for C60). Now the F-factors obtained for individual compounds at the fixed wavelengths will be used for calculation of fields E_m and E_b in the heterostructure.

2.4 Built-in fields in the heterostructure

Fig. 2.2c shows 1ω and 2ω spectra of heterostructure ITO-CuPc-C60-Al at $U_m = 8$ V. Here, again in the spectral area of CuPc (600-800 nm) the curves 1ω and 2ω have opposite signs but in the spectral area of C_{60} (350-750 nm) their signs are the same. Unfortunately, now a distribution of the amplitude of a.c. field E_m over the layers is not known because the electric induction may not be conserved along the heterostructure due to a possible accumulation of free charges, for example, at the boundary between CuPc and C_{60}. However, the F-factors for both materials are already found and from Eq. (2.1) and the values of $\Delta A_{m,2w}$ at $\lambda = 728$ and 368 nm in Fig. 2.2c the amplitudes $E_m = 47$ V/μm (for CuPc) and $E_m = 82.5$ V/μm (for C_{60}) are calculated, see the Table. Correspondingly, assuming a simplified model for a homogeneous field across the CuPc and C_{60} layers, we find an a.c. voltage drops U_m on each layer to be 2.55 V and 5.75 V and the sum of the two (8.25 V) appears to be close to the applied voltage of 8 V. Some difference may be attributed to the mentioned simplification and inaccuracy of CuPc and C_{60} layer thickness. Finally, again with the help of Eq. (2.4), the amplitudes of the built-field $E_b = 14.7$ V/μm (CuPc) and – 21.8 V/μm (C_{60}) have been found together with the voltage drops on the corresponding layers U_b(CuPc) = 0.81 V and $U_b(C_{60}) = -1.53$ V (see the Table). The direction of the two fields were again verified by applying a low external voltage $U_0 = \pm 1.2$ V. The bias voltage of + 1.2 V with respect to the grounded ITO electrode increases the amplitude of $\Delta A_{m,\omega}$ in the spectral range of CuPc but $U_0 = -1.2$ V decreases it. It means that in CuPc layer the direction of E_0 coincides with direction of the built-in field E_b (at $U_0 = 0$ from Al to ITO). On the contrary, in the C_{60} layer, the built-in field at $U_0 = 0$ is directed from ITO to Al. We believe that the opposite transient photovoltages observed in [14] in CuPc / C_{60} and C_{60} / CuPc heterostructures should be discussed in terms of the opposite built-in fields investigated here.

3. DISCUSSION AND CONCLUSION

The experimental data in the Table allows us to draw an approximate scheme of the built-in field in the bulk of heterostructure. In contrast to Inset to Fig. 2.1, all the layers shown in Fig. 3.1b are in contact with each other i.e. they are in thermodynamic equilibrium. It is essential that a potential difference between the electrodes is solely dictated by the work functions of Al and ITO [15] (the chemical interaction between the semiconductors and electrodes is neglected).

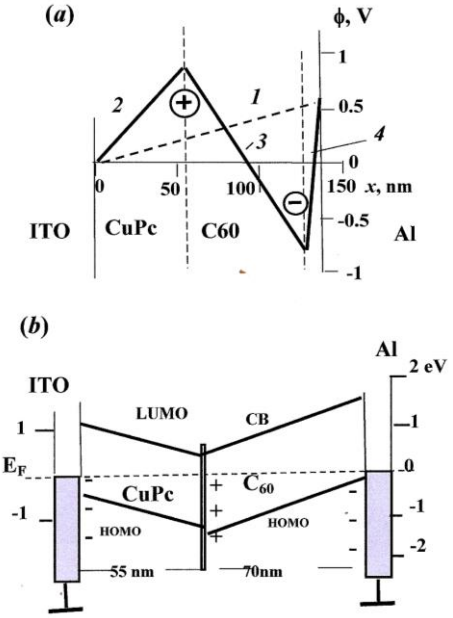

Fig. 3.1 – *a*) Simplified diagram of the potentials and built-in fields with the scales corresponding to the experimentally measured average fields in the bulk of the CuPc and C_{60} layers. CB means the bottom of the conduction band; Potential $\phi(x)$ is plotted versus a distance x along the heterostructure, solid line 2-3-4 with two fractures shows a realistic situation with signs "+" and "–" marked off the places of charge accumulation. Line 1 is just a guide correspondent to $\phi_{Al} = +0.6$ eV and vertical dash line marks off a contact layer thickness (not in scale). *b*) Scheme of electron energy in the heterostructure ITO-CuPc-C60-Al in thermodynamic equilibrium; E_F – Fermi level

For discussion of built-in fields, it is convenient to operate with electric potential. First of all we fix zero potential ($\phi_{ITO} = 0$) at the Ohmic contact ITO / CuPc for holes [16]. Then the Al potential in Fig. 3.1a $\phi_{Al} = -4.2 - 4.8 = +0.6$ eV is fixed on the ordinate axis. Here all potentials $\phi(x)$ and distances x along the heterostructure are shown in precise correspondence with the experimental data in the Table. For a guide, the slope of line 1 corresponds to the field between electrodes in

vacuum, $E_{vac} = \phi_{Al} / ed_e$ where $d_e = 125$ nm is equal to the thickness of our heterostructure. Then, the voltage $U_b = 0.81$ V from the last column of the Table corresponds to a potential $\phi_1 = 0.81$ eV at $x = 55$ nm (edge of CuPc layer) and line 2 shows the slope of the potential, i.e. $E_b = + 14.7$ V/μm. Next, the line 3 is drawn according to the negative field $E_b = - 21.8$ V/μm in C_{60} with potential difference $\phi_2 = - 1.53$ eV dropped between $x = 55$ nm and ≈ 125 nm (very near to the edge of C_{60} layer). Finally, according to the Volta rule, line 4 terminates the scheme at $\phi_{Al} = + 0.6$ eV, manifesting a very strong slope (contact field) between C_{60} and Al. This strong field inevitably appears at the high energy barrier at C_{60} / Al contact which is shown in Fig. 3.1a but not at the ITO / CuPc Ohmic contact [16]. Therefore, the electron energy scheme in Fig. 3.1b seems to be feasible.

Since the d.c. built-in fields in the bulk of CuPc and C_{60} are opposite and diverge from each other, we can calculate the excess density of accumulated positive charges (holes) at the CuPc / C_{60} interface mostly compensated by a lack of holes at the C_{60} / Al contact:

$$\sigma = \varepsilon_0 \Delta(\varepsilon E_b) = \varepsilon_0 (\varepsilon_{CuPc} E_{b,CuPc} - \varepsilon_{C60} E_{b,C60}) \quad (3.1)$$

where ε_0 is vacuum dielectric constant, $\varepsilon_{CuPc} \approx 4$ and $\varepsilon_{C60} \approx 4.5$. As $E_{b,C60}$ is negative, the charge density $\sigma = 1.4 \cdot 10^{-3}$ C/m^2 is very large, as compared, for example, to earlier data on organic light-emitted diodes [7]. We believe that this charge is brought about by the holes trapped by multiple surface states at the CuPc / C_{60} boundary.

In conclusion, the spectroscopic electroabsorption technique developed theoretically and experimentally is presented as a tool for measurements of a.c. and d.c (built-in) fields in absorbing layers of multilayer organic heterostructures. For the measurements of the both fields the electroabsorption signal was detected, correspondingly, at the fundamental and double frequency of the applied electric voltage. This spectroscopic technique was used to investigate a solar cell type heterostructure ITO-CuPc-C_{60}-Al that includes active layers of copper phthalocyanine (CuPc, donor) and fullerene (C_{60}, acceptor) between ITO and Al electrodes. First, there were prepared two simpler structures ITO-CuPc-Al and ITO- C_{60}-Al and their built-in fields were measured in the bulk of CuPc and C_{60} layers. Then, so-called *F*-factors (parameters of individual materials) were found for CuPc and C_{60}, that was necessary for a subsequent study of the fields in the heterostructure. Finally, the built-in fields were measured in the CuPc and C_{60} layers within the heterostructure and it has been found that those fields had opposite direction, from Al to ITO for CuPc and from ITO to Al for C_{60}. This unexpected result is related to accumulation of the excess holes trapped at the CuPc / C_{60} interface and a lack of holes at C_{60} / Al interface; the potential diagram of the case is presented. We believe that, for further experiments with photovoltaic heterostructures, it should be taken into consideration that opposite built-in fields, which control a drift of charge carriers to electrodes, could either increase or reduce the power efficiency of a particular photovoltaic device in dependence of cell geometry and material.

ACKNOWLEDGEMENTS

The work was supported by Russian Foundation for Basic Research (project No 12-02-00214a). The authors are grateful to Drs. S.P. Palto and S.V. Yablonskii (Institute of Crystallography, RAS) for the help in experiment and fruitful discussions.

REFERENCES

1. P. Peumans, A. Yakimov, S.R. Forrest, *J. Appl. Phys.* **93**, 3693 (2003).
2. B. Kippelen, J-L. Bredas, *Energ. Environ. Sci.* **2,** 251 (2009).
3. S.R. Cowan, N. Banerji, W.L. Leong, A.J. Heeger, *Adv. Funct. Mater.* **22**, 1116 **(**2012).
4. G.G. Malliaras, J.R. Salem, P.J. Brock, J.C. Scott, *J. Appl. Phys.* **84**, 1583 (1998).
5. L.M. Blinov, *Non-centersymmetric Langmuir-Blodgett Film* (*Soviet Scientific Reviews A: Physics Reviews*), I.M. Khalatnikov Ed., **12**, Part 1, (Harwood Acad. Publ.: London: 1989).
6. L.M. Blinov, S.P. Palto, S.G. Yudin, *J. Mol. Electron.* **5**, 45 (1989).
7. I.H. Campbell, M.D. Joswick, I.D. Parker, *Appl. Phys. Lett.* **67**, 3171 (1995).
8. L.M. Blinov, V.V. Lazarev, S.G. Yudin, S.P. Palto, *JETP Let*. **95**, 160 (2012).
9. C.-F. Lin, M. Zhang, S.-W. Liu, T.-L. Chiu, J-H. Lee, *Int. J. Mol. Sci.* **12**, 476 (2011).
10. S.W. Cho, J.H. Seo, C.Y. Kim, K.-H. Yoo, K. Jeong, C.-N. Whang, *Appl. Phys. Lett.* **88**, 151103 (2006)
11. M. Muccini, R. Zamboni, C. Taliani, L. Blinov, *Frenkel and Charge Transfer Excitons in solid C60* (Eds. H. Kuzmany, J. Link, M. Mehring, S. Roth), (World Scientific Publ. Co: Singapore: 1996).
12. W. Liptay, *In Modern Quantum Chemistry* (Ed. O. Sinanoglu), (Acad. Press: New York: 1965).
13. S.P. Palto, A.V. Sorokin, A.A. Tevosov, S.G. Yudin, *Opt. Spectr.* **98**, 574 (2005).
14. Q.L. Song, C.M. Li, M.L. Wang, X.Y. Sun, X.Y. Hou, *Appl. Phys. Lett.* **90**, 071109 (2007).
15. L.D. Landau, E.M. Lifshits, *Electrodynamics of Continuum Media* (Pergamon: London: 1960).
16. A.K. Mahapatro, S. Ghosh, *Appl. Phys. Lett.* **88**, 4840 (2002).